Atmos. Chem. Phys. Discuss., 7, 14675–14706, 2007
www.atmos-chem-phys-discuss.net/7/14675/2007/

Atmospheric Chemistry and Physics Discussions

Introduction of prognostic rain in ECHAM5: design and Single Column Model simulations

R. Posselt and U. Lohmann

Institute for Atmospheric and Climate Science, ETH Zurich, Universitaetsstrasse 16, 8092 Zurich, Switzerland

Received: 14 September 2007 – Accepted: 12 October 2007 – Published: 15 October 2007

Correspondence to: R. Posselt (rebekka.posselt@env.ethz.ch)

Abstract

Prognostic equations for the rain mass mixing ratio and the rain drop number concentration are introduced into the large-scale cloud microphysics parameterization of the ECHAM5 general circulation model (ECHAM5-RAIN). For this a rain flux from one level to the next with the appropriate fall speed is introduced. This maintains rain water in the atmosphere to be available for the next time step. Rain formation in ECHAM5-RAIN is, therefore, less dependent on the autoconversion rate than the standard ECHAM5 but shifts the emphasis towards the accretion rates in accordance with observations. ECHAM5-RAIN is tested and evaluated with two cases: the continental mid-latitude ARM Cloud IOP (shallow frontal cloud case – March 2000) and EPIC (a marine stratocumulus study – October 2001). The prognostic equations for rain hardly affect the amount and timing of precipitation at the surface in different Single Column Model (SCM) simulations for heavy precipitating clouds because heavy rain depends mainly on the large-scale forcing. In case of thin, drizzling clouds (i.e., stratocumulus), an increase in surface precipitation is caused by more sub-time steps used in the prognostic rain scheme until convergence is reached. Cloud microphysical quantities, such as liquid and rain water, are more sensitive to the number of sub-time steps for light precipitation. This results from the decreasing autoconversion rate and increasing accretion rate.

1 Introduction

Clouds and precipitation play an important role in the hydrological cycle of the earth. Changing precipitation patterns due to climate change will result in shifted vegetation zones, will have an influence on water quality, soil structure/erosion and runoff into rivers and oceans (Hatfield and Prueger, 2004). Through feedback processes, these changed precipitation rates have an impact on cloud formation and microphysical processes which, on their part, influence the precipitation rates. Recently, the impact of aerosol particles resulting from human activity on cloud and precipitation formation received a lot of attention (e.g., Denman et al., 2007; Lohmann and Feichter, 2005; Penner et al., 2006; Storelvmo et al., 2006). Thus, a proper treatment of cloud microphysical processes in models, especially in General Circulation Models (GCM) like the ECHAM5, is necessary to obtain reliable predictions of the aerosol indirect effects (Twomey, 1974; Albrecht, 1989) on clouds and precipitation and hence, on the radiative budget of the earth.

The formation of precipitation in a GCM is closely related to the parameterization of cloud microphysical processes. An assumption that is widely used in GCMs is that the sedimentation of rain drops is very fast compared to the model time step. Hence, all precipitation particles formed within one time step will fall through the whole vertical column within the same time step. On the way down, they can evaporate and participate in the accretion process. The disadvantage of this concept is that, for each time step, the rain drops first have to be newly produced by autoconversion. This process is determined less important in the atmosphere than accretion of cloud droplets by rain (Wood, 2005). The evaluation of profiles from in-situ microphysical measurements from 12 flights over the ocean (close to the UK) by Wood (2005) revealed that accretion is the most relevant process for drizzle production in the lower 80 % of the cloud. In the upper 20 % of the cloud, autoconversion and accretion are equally important. Thus, the concept of diagnostic precipitation weight the in-cloud conversion processes unrealistically by putting too much emphasis on the autoconversion rate.

The motivation for this study is to investigate the influence of giant cloud condensation nuclei (GCCN) on the warm rain formation. GCCN are regarded as aerosol particles larger than 5 – 10 µm. Seeding GCCN into a non-precipitation cloud (due to high amounts of anthropogenic aerosol particles) might initiate precipitation due to an enhanced collection of small cloud droplets by the larger drops that originate from GCCNs. Therefore, GCCN could counteract the aerosol indirect effects (e.g., Johnson, 1982; Feingold et al., 1999; Rosenfeld et al., 2002). The resulting precipitation can be regarded as drizzle as the drops are rather small and the total precipitation rate is low.

Therefore, the assumption that all rain is removed within one model time step might not hold true for these clouds. Lower fall speeds in the model imply that part of the rain water is kept in the atmosphere and is available for the next model time step. To keep track of the rain water in the atmosphere, rain has to be treated prognostically in the model instead of diagnostically.

Several large scale microphysics schemes (e.g., Lohmann and Roeckner, 1996; Rotstayn, 1997) treat precipitation diagnostically so that all precipitation is removed from the atmosphere within one model time step. This method was put forward by Ghan and Easter (1992) who showed that using diagnostic precipitation allows for longer model time steps without significantly changing the temporal evolution of cloud water and ice. Nevertheless, some GCMs treat the precipitation prognostically by including sedimentation of precipitation. Fowler et al. (1996) implemented a one-moment microphysics scheme into the CSU[1] GCM accounting for changes in water vapor, cloud water and cloud ice, rain and snow. The microphysical processes include condensation/evaporation of cloud water, deposition/sublimation of cloud ice, evaporation of rain/snow, melting of snow and freezing of rain, collisions between the hydrometeor classes (i.e., autoconversion, accretion) and the Bergeron-Findeisen process. The precipitation processes including the sedimentation of rain and snow are treated on a small time step (2 min) using a time-splitting method. A mass-weighted fall speed for rain and snow is applied in the sedimentation scheme. Lopez (2002) incorporated a large-scale cloud scheme into Meteo France's operational global model ARPEGE[2]. It uses cloud condensate and precipitation as prognostic variables. Microphysical processes include condensation/evaporation of cloud condensate, evaporation of precipitation, autoconversion and accretion. The sedimentation of precipitation is done in a simple semi-Lagrangian framework assuming constant fall velocities for rain ($5\,\mathrm{ms}^{-1}$) and snow ($0.9\,\mathrm{ms}^{-1}$). The implementation of moist processes including rain sedimen-

[1] Colorado State University

[2] Action de Recherche Petite Echelle et Grande Echelle

tation into the EULAG[3] model is described by Grabowski and Smolarkiewicz (2002). The EULAG model is a multi-scale model covering cloud resolving scales up to global scales. The microphysical parameterizations (Grabowski, 1998) are given for cloud condensate and precipitation and include condensation of water vapor, autoconversion of cloud condensate into precipitation and accretion of cloud condensate by precipitation, as well as deposition/evaporation of precipitation. The cloud microphysical processes are evaluated on time steps appropriate for the considered problem which can be smaller than the model dynamics time step. The sedimentation of precipitation is determined by a one-dimensional flux-form advection scheme. Global simulations deploy time steps of 30 s for a second-order explicit scheme (MPDATA, Smolarkiewicz and Margolin, 1998) or 600 s for an implicit upwind scheme for the precipitation simulations.

The present paper focus on the introduction of prognostic equations for the rain mass mixing ratio and the rain drop number concentration into the large-scale cloud scheme within ECHAM5. An explicit fall speed for the sedimentation of rain drops is derived that depends on the rain drop size. The precipitation processes are calculated on smaller time steps using a time-splitting method. Thus, a better representation of the microphysical processes in which rain is involved is achieved. In case of the applied explicit numerical scheme for the sedimentation, the time-stepping is also necessary to assure numerical stability. As this study focus on warm phase precipitation formation, snow is still treated diagnostically for the moment. GCCN are not yet included.

Results from a single column simulation with the newly introduced prognostic rain will be presented. Single column model (SCM) simulations are conducted with a case from the EPIC[4] stratocumulus study that took place in September and October 2001 in the eastern Pacific (off the coast of Ecuador and Peru) (Bretherton et al., 2004). A second

[3] EUlerian - semi-LAGrangian model (Smolarkiewicz and Margolin, 1997)

[4] Eastern Pacific Investigation of Climate Processes

SCM case is derived from ARM IOP[5] measurements. The shallow frontal cloud case of the Cloud IOP (Xu et al., 2005) that took place in March 2000 at the ARM Southern Great Plain Site in Oklahoma is chosen. For these two cases, changes in precipitation and the cloud properties due to the introduction of the prognostic equations for rain will be investigated. The results from these simulations will be compared to ECHAM5-HAM (Lohmann et al., 2007), which includes a coupling between aerosols and cloud scheme, and to observations from EPIC and ARM.

2 Model description

2.1 The general circulation model ECHAM5

The ECHAM5-GCM is based on the ECMWF model and has been further developed at the Max-Planck-Institute for Meteorology in Hamburg. Within ECHAM5 the prognostic equations for temperature, surface pressure, divergence and vorticity are solved on a spectral grid with a triangular truncation (Roeckner et al., 2003). The used ECHAM5-HAM version comprises a two-moment cloud scheme with prognostic equations for cloud water (ice) and cloud drop (ice crystal) number concentration as well as detailed cloud microphysics (Lohmann and Roeckner, 1996; Lohmann et al., 1999, 2007). Within the aerosol module HAM (Stier et al., 2005), atmospheric aerosol distributions are represented by a double moment scheme consisting of a superposition of 7 log-normal distributions of different size ranges, solubilities, and chemical constituents. For the simulations in this study the statistical cloud cover scheme of Tompkins (2002) is used.

[5]Atmospheric Radiation Measurement program, Intensive Operational Period

2.2 Prognostic equations for rain

Within ECHAM5-HAM, rain is treated diagnostically and the total rain water is removed from the model after one time step (as surface precipitation flux) or by evaporation in the sub-saturated air below the cloud. This approach is only true for relatively large rain drops (r>100 µm). Smaller drops, i.e., drizzle (25 µm<r<100 µm), also sediment but may not reach the surface within one time step. To account for this behavior, prognostic equations for rain are introduced with the following processes. Firstly, a rain flux enters a given level from above and leaves this level due to the sedimentation of rain drops (sed). New rain drops form by autoconversion of cloud droplets (aut). The rain drop number decreases by self collection (scr) of rain drops. An increase in rain water is caused by accretion of cloud droplets by rain drops (acr), whereas, the evaporation of rain (evpr) in the sub-saturated air below cloud leads to a decrease in rain water mixing ratio. A further source of rain drop mass and number is the melting of snow (mls). A further source for rain water and number is the direct activation of GCCN (nucr) into rain drops which is not yet included. The rates of rain water mixing ratio $\partial q/\partial t$ and rain drop number concentration $\partial N/\partial t$ due to these processes are summarized in Eqs. (1). Q and P denote changes in the rain water mixing ratio and in the rain drop number concentration, respectively and the cloud and precipitation fractions are denoted with b_c and b_r, respectively.

$$\frac{\partial q}{\partial t} = Q_{\mathrm{nucr}} + b_c\,(Q_{\mathrm{aut}} + Q_{\mathrm{acr}}) - (1 - b_c)\,Q_{\mathrm{evpr}} + b_r\,(Q_{\mathrm{mls}} + Q_{\mathrm{sed}}) \tag{1a}$$

$$\frac{\partial N}{\partial t} = P_{\mathrm{nucr}} + b_c\,(P_{\mathrm{aut}}) + b_r\,(P_{\mathrm{mls}} - P_{\mathrm{scr}} + P_{\mathrm{sed}}) \tag{1b}$$

Except for the rain flux, all microphysical processes are already part of ECHAM5-HAM and are now also included in the prognostic equations for rain. The parameterization of the microphysical processes (*aut* and *acr*) are taken from Khairoutdinov and Kogan (2000). In case of evaporation, it is assumed that all rain drops shrink which results in a changed mass mixing ratio but constant rain drop number concentration.

The cloud cover b_c is calculated with the statistical cloud cover scheme by Tompkins (2002). At beta distribution is assumed as the probability density function (PDF) for the total water q_t (water vapor + cloud water + cloud ice) of the grid box. The cloud cover is then defined as the integral over the saturated part of the PDF (i.e., for $q_t > q_s$, with q_s denoting the saturation specific humidity). The precipitation fraction b_r is determined by the cloud fraction of the precipitating cloud. Following the precipitation on its way from the cloud to the surface a maximum overlap of b_r is assumed. Snow is still treated diagnostically, i.e. all snow will be removed from the atmosphere within one model time step either by melting (generating rain), by sublimation or as surface precipitation. To be consistent, snow should also be treated prognostically but this is beyond the scope of this study. For future studies prognostic snow will be considered as well. Because only the snow mass is given the size of the melted snow is assumed to be 25 µm. This size is chosen according to the separation size for cloud droplets and rain drops proposed by Khairoutdinov and Kogan (2000). The calculation of the incoming and outgoing rain fluxes is described in the next section.

2.3 Rain flux and rain drop sedimentation

The sedimentation of the rain drops and, with it, the rain flux from one model level to the next is treated as a vertical 1D-advection with the mass weighted fall velocity v_m (positive in downward direction) of the rain water mass mixing ratio q [kg kg^{-1}] and rain drop number concentration N [m^{-3}], respectively. The advection equation is expressed in flux form to account for changes in rain water mass and number with changing density, i.e., with height. Therefore, it is more convenient to express the number of rain drops as mixing ratio $n = N/\rho_a$ (n in [kg^{-1}]). For simplicity, the same velocity v_m is used for rain mass and number mixing ratio.

ACPD
7, 14675–14706, 2007

R. Posselt and U. Lohmann

EGU

$$Q_{\text{sed}} = \left.\frac{\partial q}{\partial t}\right|_{\text{sed}} = \frac{1}{\rho_a}\frac{\partial}{\partial z}(\rho_a\, q\, v_m) \tag{2a}$$

$$P_{\text{sed}} = \left.\frac{\partial n}{\partial t}\right|_{\text{sed}} = \frac{1}{\rho_a}\frac{\partial}{\partial z}(\rho_a\, n\, v_m) \tag{2b}$$

The numerical solution is found by an upstream scheme in space and a forward scheme in time. The decision for this explicit scheme has several reasons. First of all, the scheme is mass conserving by definition which is very important when dealing with cloud microphysics. Furtheron, the explicit scheme is quite easy to implement in the given structure of the ECHAM5-HAM large-scale cloud scheme. The microphysical processes are treated sequentially, i.e., one after the other, in each level starting from the top level to the bottom. The sedimentation into the next level takes place after the cloud microphysical processes. This "stepwise" sedimentation requires the determination of outgoing and incoming quantities separately (i.e., in level i: determine what is going out of level i and what is getting into level $i+1$). The usage of implicit schemes or more sophisticated explicit schemes would require a total restructuring of the model with a separation between microphysical processes and sedimentation. This in turn would require an extensive retuning of the model which is not wanted for this study. Nevertheless, the explicit scheme is very diffusive and has low spatial and temporal discretization abilities. Therefore, once it is shown that the implementation of the prognostic rain scheme is beneficial for the representation of clouds and precipitation, a more sophisticated sedimentation scheme will be implemented.

To calculate the actual rain flux from one model level to the next an approach for the fall velocity of rain drops is introduced. The starting point is the flux density approach used by Srivastava (1978) (his Eq. (48) for the mass flux).

$$\mathfrak{F}_m = (q\,\rho_a)\cdot v_m = \int_0^\infty m\, f(m)\, v_s(m)\, dm \tag{3}$$

ACPD
7, 14675–14706, 2007

Thereby, q denotes the rain water mass mixing ratio, ρ_a the air density, and v_s denotes the terminal velocity of a single rain drop. For the rain drop size distribution f an exponential distribution – as was first put forward by Marshall and Palmer (1948) – is assumed.

$$f(D) = N_D \exp(-\lambda D) \tag{4}$$

Grabowski (1999) suggested the following expression for λ and N_D using the model variable q.

$$\lambda = \frac{1}{D_0} = \left(\pi \rho_w \frac{N_D}{\rho_a q}\right)^{\frac{1}{4}} \tag{5}$$

Thereby, ρ_w and ρ_a are the density of water and air, respectively. In the following, D_0 will be used as distribution parameter instead of λ. In contrast to the Marshall-Palmer distribution and to the distribution by Grabowski (1999), the parameter N_D is not constant but determined by the number of rain drops N in the model so that the expressions for N_D and D_0 become

$$N_D = \frac{N}{D_0} \qquad \text{and} \qquad D_0 = \left(\pi \rho_w \frac{N}{\rho_a q}\right)^{-\frac{1}{3}}. \tag{6}$$

In models, it is more convenient to work with the drop mass instead of the droplet diameter. With $m = \frac{1}{6}\pi \rho_w D^3 = (c \cdot D)^3$ and $f(m) = f(D)\frac{dD}{dm}$ the rain drop distribution takes the form of a more generalized exponential (i.e., Weibull) distribution which is used in Eq. (3):

$$f(m) = \frac{N}{3}\left(\frac{m}{m_0}\right)^{\frac{1}{3}} \exp\left[-\left(\frac{m}{m_0}\right)^{\frac{1}{3}}\right]\frac{1}{m} \tag{7}$$

The distribution parameters m_0 and D_0 are related to the mean mass $\overline{m}$ and mean diameter $\overline{D}$ of the rain drop size distribution as follows:

$$\overline{m} = \frac{\rho_a q}{N} = 6\, m_0 \quad \text{and} \quad \overline{D} = \sqrt[3]{6}\, D_0 \tag{8}$$

ACPD
7, 14675–14706, 2007

Furthermore, to solve Eq. (3) it is convenient to take advantage of the moments $M^{(k)}$ of the size distribution $f(m)$. In case of a Weibull distribution (such as Eq. (7)), the moments can be expressed with the help of the Gamma function $\Gamma(x)$:

$$
\begin{aligned}
M^{(k)} &= \int_0^\infty m^k\, f(m)\, dm = N\, m_0^k\, \Gamma(3k+1) \\
&\overset{3k\in\mathbb{N}}{=} N\, m_0^k\, (3k)!
\end{aligned}
\tag{9}
$$

In terms of moments, the number concentration N can be expressed as $M^{(0)}$ and the rain water mixing ratio $q = M^{(1)}/\rho_a$.

The last important ingredient for Eq. (3) is the fall velocity of a single rain drop v_s which is approximated according to Rogers et al. (1993).

$$
v_s(D) = \begin{cases} a_1\, D\, [1 - \exp(-a_2\, D)] & D \le 745\,\mu m \\ b_1 - b_2\, \exp(-b_3\, D) & D \ge 745\,\mu m \end{cases}
\tag{10}
$$

with D denoting the diameter of the rain drop and the constants $a_1 = 4000\,\mathrm{s}^{-1}$, $a_2 = 12000\,\mathrm{m}^{-1}$, $b_1 = 9.65\,\mathrm{m\,s}^{-1}$, $b_2 = 10.43\,\mathrm{m\,s}^{-1}$, and $b_3 = 600\,\mathrm{m}^{-1}$. Unfortunately, this two-splitted formulation is problematic as the solution of the mass flux equation with the method of the moments requires one equation for v_s for the whole size range. To circumvent this problem, an additional term was added to the second equation of (10) to obtain a better fit to the first equation at lower rain drop sizes. This leads to a lower accuracy for lower sizes. Because the fall velocities are rather small, the drops in that size range would not fall very far within one model time step. Therefore, this loss of accuracy is negligible for the purpose of this application. The resulting equation for the fall velocity of a single rain drop is given by:

$$
v_s(D) = b_1 + (b_2 - b_1)\, exp(-5\, b_3\, D) - b_2\, exp(-b_3\, D)
\tag{11}
$$

The fall velocities of a single drop according to Eq. (10) (black dotted and dashed lines) as well as according to Eq. (11) are shown in Fig. 1 (upper panel).

ACPD

7, 14675–14706, 2007

Introduction of prognostic rain in ECHAM5

R. Posselt and U. Lohmann

EGU

Inserting the rain drop size distribution (7) and equation (11) into the mass flux equation (3) and using the definition of the moments (Eq. (9)) leads to the following expression for the mean fall velocity v_m:

$$v_m = \frac{\mathfrak{F}_m}{\rho_a\, q} = \begin{cases} 4\,\frac{b_v}{c}\, m_0^{\frac{1}{3}} & \text{for } m_0 \ll m_v \\ b_1 & \text{for } m_0 \gg m_v \end{cases} \tag{12}$$

The constant b_v is given by $b_v = b_3\,[b_2 - 5(b_2 - b_1)]$. The critical mass parameter m_v has the value 0.122×10^{-6} kg with the corresponding mean rain drop size of $\overline{D}_v$ = 1118.7 µm.

The rain drop fall velocity v_m is a function of the distribution parameter m_0 and, therefore, a function of the mean size of a rain drop in contrast to constant fall velocities (Lopez, 2002) or mass-weighted fall velocities (Fowler et al., 1996). The asymptotic solutions for the fall velocity v_m as a function of D_0 for small and large drops (black dotted and dashed lines) are shown in Fig. 1 (lower panel). The red line represents the values used for the fall velocity for q and N.

If using fall speeds for the rain drops within an explicit numerical scheme, the Courant-Friedrichs-Levy (CFL) criterion for numerical stability has to be obeyed. The CFL criterion is violated if relatively large rain drops fall too fast/too far down and, therefore, miss a model level resulting in negative rain drop mass and number. To prevent this (and the resulting chaotic behavior of the model) a reduction of the time step is necessary. Because it is computationally too expensive to be applied for the whole model, only the time step in the cloud microphysics routine is decreased. Only processes directly connected to the precipitation formation, such as autoconversion, accretion, and sedimentation are calculated using the smaller time step which also leads to a better representation of the precipitation formation via accretion. All other processes (i.e., the ice microphysics) are still calculated with the longer model time step. This requires some rearrangement in the sequence of the microphysical calculations. Given the non-linear structure of most of the microphysical parameterizations this already changes the results for the cloud and precipitation formation. For this paper, the number of those smaller time steps is fixed to constant values (e.g., 3, 10, 30, ...) that are valid for the whole simulation. Nevertheless, it is possible that the fall velocity is so high that the rain drops would fall too far (especially, if they reach the lowermost model levels). For that reason, the maximum fall velocity within a level is limited by the grid velocity $v_{max} = \Delta z / \Delta t$. v_{max} is necessary for numerical reasons although it does slow the sedimentation artificially, especially for larger time steps.

2.4 Break-up

Spontaneous break-up for drops larger than 5 mm happens very rarely in real clouds as the collisional break-up prevents drop growth to these sizes (Pruppacher and Klett, 1997). In the model, break-up processes, like the collisional break-up, are not considered. Therefore, drops can grow to rather large and unrealistic sizes. To prevent this, a simple approach for the spontaneous break-up is introduced. If the number of drops larger than 5 mm exceeds 1 % of the total rain drop number concentration then the rain drop distribution is changed by increasing the total rain drop number. The corresponding size distribution after the break-up has the distribution parameter $D_{0,B}$.

$$\frac{1}{N}\int_{D_B}^{\infty} f(D)dD = \exp\left(-\frac{D_B}{D_{0,B}}\right) > 0.01 \tag{13}$$

As soon as $D_0 \geq D_{0,B} = 1085.7\,\mu\text{m}$, break-up will occur. The new rain drop number concentration is then determined by $N_B = (\rho_a q)/m_{0,B}$, where $m_{0,B}$ is the corresponding mass to the break-up distribution diameter $D_{0,B}$.

ACPD

7, 14675–14706, 2007

EGU

3 Results and discussion

3.1 Model setup

The following simulations are conducted with the Single Column Model (SCM) version of ECHAM5 using 31 model levels with the uppermost layer at 10 hPa. A simulation time step of 15 min is applied. The simulations described employ the cloud cover scheme by Tompkins (2002). The boundary conditions for the SCM are taken from forcing datasets provided by the field campaign data archives (see references for the websites).

One simulation was completed with ECHAM5-HAM which is then compared to four simulations of the altered version ECHAM5-RAIN with different numbers of sub-time steps. Additionally, all simulations are compared to observations.

The discussion of the results focuses on the evolution of cloud and precipitation quantities like the precipitation flux at the surface, cloud and rain water content, cloud cover and microphysical conversion rates. Thereby changes due to the different number of sub-time steps are evaluated with regard to finding the optimal number of sub-time steps for GCM simulations where a compromise between accuracy and computational time has to be found. Furtheron, the SCM simulations are compared to the observational data from the considered measurement campaigns. One has to bear in mind that perfect agreement between simulations and observations cannot be reached. Forcing the SCM with observations usually lacks some advective tendencies (e.g., hydro-meteor advection) to describe transport in and out of the model column. Therefore, the conditions at the measurement site cannot be fully reproduced by the model. Furthermore, measurements are always subject to uncertainties which also contribute to differences between model and observations. Nevertheless, the SCM is a good tool to test the new prognostic rain scheme and evaluate the behavior for different number of sub-time steps.

ACPD
7, 14675–14706, 2007

3.2 EPIC 2001

EPIC, the Eastern Pacific Investigation of Climate Processes (in the coupled ocean-atmosphere system) took place in September and October 2001. Besides investigating deep convection and ocean mixing, one goal was to study stratocumulus clouds and boundary layer processes. During a 2 week period in October 2001, ship-based remote sensing and ground-based measurements were taken to characterize the vertical structure of the atmospheric boundary layer and to understand the physical processes behind the stratocumulus cloud albedo. A characteristic of the campaign was an extensive stratocumulus deck which was usually organized into mesoscale cellular structures (Bretherton et al., 2004).

The EPIC Integrated Dataset of the stratocumulus study was used to force the ECHAM5 SCM. The profiles of temperature, specific humidity and horizontal wind speed were obtained from radio soundings during the campaign. The large-scale forcings, i.e. temperature and specific humidity advection, as well as the large-scale subsidence, were derived from ECMWF reanalysis data. Additionally, a cloud condensation nuclei concentration of 150 cm^{-3} is prescribed to obtain a cloud drop number concentration of 100 – 130 cm^{-3} which was observed during EPIC.

3.2.1 Comparison to observations

The mean values for the precipitation at the surface and at cloud base, the total cloud cover and the liquid, rain and total water path (LWP, RWP and TWP=LWP+RWP) averaged over the whole simulation period for the observations and the SCM simulations are summarized in Table 1.

Our first attention is drawn to the development of precipitation and the rain water content in the atmosphere. On average, the ECHAM5 simulations precipitate less at cloud base as well as at the surface than the observations (see Table 1). As can be seen in Fig. 2, ECHAM5 generally captures the temporal evolution of the precipitation quite well. Some of the measured peaks are reproduced correctly with regard to the

ACPD
7, 14675–14706, 2007

timing but the precipitation amount does not fit. On the other hand, there are several rain events that the model totally misses or that are simulated but not observed. For the surface precipitation the relative differences are larger than at cloud base (see Table 1) which results from too weak evaporation. In the simulations about 55 – 60 % of the rain water evaporates below cloud base, whereas the observed evaporation ratio is 85 % (Bretherton et al., 2004).

Reasons for the differences between observed and simulated rain can be due to the forcing data set so that the model is not able to reproduce the meteorological conditions correctly. Furthermore, ECHAM5 might be missing some essential processes (e.g., embedded convection) that result in larger precipitation amounts in the observations. Another factor is the large uncertainty of a factor 2–3 of the radar retrievals (Bretherton et al., 2004). Thus, the difference between observation and simulation lies mostly within the uncertainties of the measurements.

Similar arguments are valid for the comparison of the total (liquid) water path (TWP) with the observed liquid water in the atmosphere. The observed liquid water path (LWP) was obtained by a microwave radiometer which differentiates between liquid and rain water in another way than ECHAM5 does. Thus, the observed LWP might also include drops which the model assumes to be rain drops. Therefore, the observations are compared with the TWP that is the sum of LWP and RWP (rain water path). The simulations show mostly a lower TWP than the observations (see Fig. 2, upper right panel and Table 1). Although the amount is not always simulated correctly the timing of the peaks is captured in most instances. It can be seen that an underestimation of the TWP leads to the missed rain events of October 18th and 20th. In this case autoconversion and accretion rates are so low that no rain water forms (see Fig. 2, lower right panel).

The underestimation of the liquid water feeds back on the cloud cover (Fig. 2, lower left panel and Table 1). Periods with overcast conditions are reproduced rather well by ECHAM5, whereas in periods with fewer clouds the cloud cover is severely underestimated. However, the overall agreement is quite good.

3.2.2 Sensitivity to sub-time step number

For high numbers of sub-time steps the model is going to converge to a final state because the maximum velocity v_{max} is not reached anymore and a lower time step length does not have a large influence on the microphysical parameterizations anymore. Sufficiently large sub-time step numbers would be in the range of 100 and more decreasing the time step length for the rain microphysics to around ten seconds. This is applicable in a SCM without problems but in a GCM high numbers of sub-time steps would increase computational time drastically. Therefore, it is necessary to limit the number of sub-time steps to take advantage of the prognostic rain but at a reasonable amount of computational cost. Comparing the SCM results for different sub-time steps gives an idea about the optimal number of sub-time steps which then will be used in the GCM simulations.

Increasing the number of sub-time steps leads to changes in the autoconversion and accretion rates. Generally, the autoconversion rate (for the whole model time step) is decreasing. The time-splitting reduces the liquid water amount that is subject to autoconversion in every sub-time step. The accretion rate itself generally increases (over the whole model time step) due to increasing rain water amounts in the atmosphere. Thus, the total conversion rate (= autoconversion + accretion rate) increases if the increase in accretion overcompensates the decrease in autoconversion. A decrease of the total conversion rate results if the decrease in autoconversion is stronger than the increase in accretion.

Figure 3 shows the vertical profiles of autoconversion, accretion and total conversion rate averaged over the whole simulation period. As expected the autoconversion rate decreases while the accretion increases. The average total conversion rate shows a slight increase which in turn results in a slight increase in precipitation and a decrease in TWP (see Table 1 and Fig. 2). The agreement with the observations gets slightly better for precipitation when increasing the number of sub-time steps but, unfortunately, worsens the agreement for the TWP. Changes in the cloud cover due to different sub-time steps are rather small and negligible.

Moisture budget consideration usually assume that the column integral of the apparent moisture sink (condensation/evaporation) equals the precipitation at the surface plus the evaporation from the surface (surface latent heat flux) (Yanai et al., 1973). Therefore the precipitation is mainly determined by the available moisture. However, in case of diminished or even suppressed autoconversion and accretion due to very low TWP as during EPIC, the precipitation formation depends not only on the available moisture but also on the amount of liquid water in the atmosphere. Liquid water has to accumulate in the atmosphere before the conversion processes can produce precipitation. Therefore, the drizzle case shows a dependence of the precipitation on the number of sub-time steps because the TWP varies with the number of sub-time steps.

Regarding the evolution of TWP and precipitation, 10 sub-time steps are sufficient to capture the essence of the collision-coalescence process. The RWP, on the other hand, would need even more sub-time steps before finally converging. However, it seems that it is not important for the surface precipitation how much rain water remains in the atmosphere as long as there is a considerable amount. Therefore, 10 sub-time steps seems to be a good compromise.

3.3 ARM IOP March 2000

The shallow frontal cloud case of the ARM Cloud IOP in March 2000 described by Xu et al. (2005) was chosen as another case to investigate the changes in the model results between ECHAM5-HAM and the new version with prognostic equations for rain. At the beginning of the IOP from 15 March to 19 March 2000, a cold front moved over the ARM site. Later in this period, a quasi-stationary low pressure system accompanied by frontogenesis characterized the weather conditions. Shallow clouds were predominant during the period but occasionally deep clouds also moved over the measurement site. Different to the drizzling EPIC case, the ARM case represents a heavy precipitating case which requires a higher numbers of sub-time steps.

The 5 day SCM simulation is forced with the meteorological conditions and corresponding large-scale horizontal advective tendencies obtained from the ARM Cloud IOP 3-hourly sounding data and surface measurements with additional data from a short-range weather prediction model (RUC-2), the NOAA wind profiler and the NOAA GOES-8 satellite.

3.3.1 Comparison to observations

Table 2 gives an overview of the mean variables (precipitation at the surface, total cloud cover, LWP, RWP and TWP) averaged over the whole simulation period for the observations and ECHAM5 simulations.

The model simulations, regardless of the ECHAM5 version and the number of sub-time steps, are much moister than the observations for the lower troposphere, especially around the cold front passage during the morning of March 16. This was already shown by Xu et al. (2005) and was explained by a missing advection of hydrometeors out of the model grid box. Thus, the cloud remains in the atmosphere much longer in ECHAM5 as well as in most other SCMs than in reality.

The temporal evolution of the rain rate is shown in Fig. 4 and summarized over the whole simulation period in Table 2. In general, ECHAM5 simulates the precipitation amount well although the model simulations overestimate the cold front precipitation at the beginning of the period. This is a direct consequence of the moister environment in the model.

The observed LWP was obtained by a millimeter cloud radar (MMCR) (Jensen and Johnson, 2006). The definition of liquid water in this case, which depends on the radar reflectivity, differs from that used in ECHAM5 (and other GCMs) (liquid water = drops with r<25 µm). Thus, the observed LWP is compared with the TWP of the model. As shown in Fig. 4 and also from Table 2, the model produces a much lower TWP than observed. The observations are characterized by relatively high TWP throughout the whole period. The SCM simulations show a quite low TWP during the cold front passage that is increasing with increasing number of sub-time steps due to an accumulation of rain water in the atmosphere (see Fig. 4, upper and lower right panel). For the rest of the period the simulated TWP agrees quite well with the observed TWP but remains on the low side.

The total cloud cover during the IOP is shown in Fig. 4 (lower left panel) and Table 2. The observed total cloud cover is derived from satellite data (GOES satellite) and correlates quite well with the rainy episodes (Fig. 4, upper left panel). The comparison with the TWP shows an inconsistency in the observations such that a non-zero TWP coincides with zero cloud cover. In general, ECHAM5 reproduces the observed cloud cover quite well. However, the simulated clouds are more persistent and the correlation with precipitation is less pronounced. Thus, the observed average total cloud cover is lower than the simulated total cloud cover (see Table 2).

3.3.2 Sensitivity to sub-time step number

Heavy precipitation is usually accompanied by large rain drops with rather high fall velocities. Hence, the treatment of such events in the given prognostic rain scheme requires a rather large number of sub-time steps to reach convergence. However, the precipitation amount itself does not depend on the amount of sub-time steps used. In this case, the amount of precipitation is determined by the large-scale forcing, i.e. by the available moisture, and the evaporation from the surface. Changes in the total water do not affect the precipitation amount but affect the residence time of water in the atmosphere. The increase in total water with a higher number of sub-time steps is mainly determined by the accumulation of rain water in the atmosphere. The cloud water does not depend on the number of sub-time steps nor does the cloud cover (Table 2).

The changes of the microphysical conversion rates are shown in Fig. 5 averaged over the whole IOP. The left panel shows that the autoconversion rate decreases with an increasing number of sub-time steps whereas the accretion rate increases. The total conversion rates show only a very weak dependence on the number of sub-time steps which is reflected in the LWP and the precipitation at the surface.

The rather heavy precipitation during the cold front passage requires even larger numbers of sub-time steps than chosen for this comparison. But the surface precipitation shows no dependence on the number of sub-time steps or even if the diagnostic or prognostic approach is used. Therefore, regarding the precipitation the choice of the sub-time step is irrelevant. That is different for the total water where the highest number of sub-time steps possible would be the best. But this is not feasible in GCM simulations.

4 Conclusions

Prognostic equations for the rain mass mixing ratio and rain drop number concentration were introduced into ECHAM5 in order to better represent the accretion process. This requires the introduction of an equation for the fall speed of rain drops. To keep the model numerically stable, a maximum vertical velocity, the so-called grid velocity, for each level was defined. With increasing number of time steps, the grid vertical velocity increases. Thus, it is applied less often making the sedimentation process more physical. With the included time-stepping, all microphysical processes associated with rain, e.g. accretion, are better represented.

The marine stratocumulus study of EPIC 2001 and the shallow frontal cloud period during the continental ARM Cloud IOP in March 2000 in Oklahoma were chosen to test the prognostic rain scheme. Five simulations were completed - one with the standard ECHAM5-HAM and four with the prognostic rain included with a different number of sub-time steps - which were compared with each other and to observations. Generally, ECHAM5-HAM and ECHAM5-RAIN reproduced the observations quite well. A major goal was to find the optimal number of sub-time steps that ensures a good representation of the rain process and that keeps the increase in computational cost reasonable. For the drizzle case the number of sub-time steps can be limited to 10 without making large errors in the estimation of the precipitation and the total water amounts. In contrast, precipitation in heavy precipitation events hardly depends on the number of sub-time steps or whether a diagnostic or prognostic rain scheme is used. Because

ACPD
7, 14675–14706, 2007

EGU

a better representation of drizzle was the reason to include a prognostic rain scheme, the future GCM simulations will be carried out with 10 sub-time steps.

The numerical scheme applied for the sedimentation of the rain drops in this study is known to be very simple and inferior. Thus, future work will also include the implementation of more sophisticated explicit or implicit numerical schemes into ECHAM5-RAIN.

Acknowledgements. The authors thank P. Spichtinger (ETH Zurich) for helpful comments and suggestions and P. Stier (Univ. of Oxford) and S. Ferrachat (ETH Zurich) for their support with the ECHAM5-HAM.

References

Albrecht, B. A.: Aerosols, cloud microphysics, and fractional cloudiness, Science, 245, 1227–1230, 1989. 14677

ARM: ARM Cloud IOP, http://iop.archive.arm.gov/arm-iop/, access: April 2007, 2000.

Bretherton, C. S., Uttal, T., Fairall, C. W., Yuter, S. E., Weller, R. A., Baumgardner, D., Comstock, K., Wood, R., and Raga, G. B.: The EPIC 2001 stratocumulus study, Bull. Amer. Meteorol. Soc., 85, 967–977, 2004. 14679, 14689, 14690

Denman, K.L., Brasseur, G., Chidthaisong, A., Ciais, P., Cox, P., Dickinson, R., Hauglustaine, D., Heinze, C., Holland, E., Jacob, D., Lohmann, U., Ramachandran, S., da Silva Dias, P., Wofsy, S., and Zhang, X.: Climate Change 2007: The Physical Science Basis. Contribution of Working Group I to the Fourth Assessment Report of the Intergovernmental Panel on Climate Change, chap. Couplings Between Changes in the Climate System and Biogeochemistry, pp. 499 – 588, Cambridge University Press, Cambridge, United Kingdom and New York, NY, USA, 2007. 14677

EPIC: EPIC Integrated Dataset, http://www.atmos.washington.edu/~caldwep/research/ScDataset/sc_integ_data_fr.htm, access: April 2007, 2005.

Feingold, G., Cotton, W. R., Kreidenweis, S. M., and Davis, J. T.: The impact of giant cloud condensation nuclei on drizzle formation in stratocumulus: Implications for cloud radiative properties, J. Atmos. Sci., 56, 4100–4117, 1999. 14677

Fowler, L. D., Randall, D. A., and Rutledge, S. A.: Liquid and ice cloud microphysics in the CSU general circulation model. Part I: Model description and simulated microphysical processes, J. Clim., 9, 489–529, 1996. 14678, 14686

Ghan, S. J. and Easter, R. C.: Computationally efficient approximations to stratiform cloud microphysics parameterization, Mon. Weather Rev., 120, 1572–1582, 1992. 14678

Grabowski, W. W.: Toward cloud resolving modeling of large-scale tropical circulations: A simple cloud microphysics parameterization, J. Atmos. Sci., 55, 3283–3298, 1998. 14679

Grabowski, W. W.: A parameterization of cloud microphysics for long-term cloud-resolving modeling of tropical convection, Atmos. Res., 52, 17–41, 1999. 14684

Grabowski, W. W. and Smolarkiewicz, P. K.: A multiscale anelastic model for meteorological research, Mon. Weather Rev., 130, 939–956, 2002. 14679

Hatfield, J. L. and Prueger, J. H.: Impacts of changing precipitation patterns on water quality, J. Soil Water Conserv., 59, 51–58, 2004. 14676

Jensen, M. and Johnson, K.: 3rd ARM Quaterly Report: Continuous Profiles of Cloud Microphysical Properties for the Fixed Atmospheric Radiation Measurement Sites (DOE/SC-ARM/P-0609), Tech. rep., Atmospheric Radiation Measurement (ARM) Program, 2006. 14693

Johnson, D. B.: The Role of Giant and Ultragiant Aerosol Particles in Warm Rain Initiation, J. Atmos. Sci., 39, 448–460, 1982. 14677

Khairoutdinov, M. and Kogan, Y.: A New Cloud Physics Parameterization in a Large-Eddy Simulation Model of Marine Stratocumulus , Mon. Weather Rev., 128, 229 – 243, 2000. 14681, 14682

Lohmann, U. and Feichter, J.: Global indirect aerosol effects: a review, Atmos. Chem. Phys., 5, 715–737, 2005, http://www.atmos-chem-phys.net/5/715/2005/. 14677

Lohmann, U. and Roeckner, E.: Design and performance of a new cloud microphysics scheme developed for the ECHAM general circulation model, Clim. Dyn., 12, 557–572, 1996. 14678, 14680

Lohmann, U., Feichter, J., Chuang, C. C., and Penner, J. E.: Prediction of the number of cloud droplets in the ECHAM GCM, J. Geophys. Res., 104, 9169–9198, 1999. 14680

Lohmann, U., Stier, P., Hoose, C., Ferrachat, S., Kloster, S., Roeckner, E., and Zhang, J.: Cloud microphysics and aerosol indirect effects in the global climate model ECHAM5-HAM, Atmos. Chem. Phys., 7, 3425–3446, 2007, http://www.atmos-chem-phys.net/7/3425/2007/. 14680

Lopez, P.: Implementation and validation of a new prognostic large-scale cloud and precipitation scheme for climate and data-assimilation purposes, Quart. J. R. Met. Soc., 128, 229–

257, http://dx.doi.org/10.1256/003590002604988789, 2002. 14678, 14686
Marshall, J. S. and Palmer, W. M.: The distribution of raindrops with size, J. Meteorol., 5, 165–166, 1948. 14684
Penner, J. E., Quaas, J., Storelvmo, T., Takemura, T., Boucher, O., Guo, H., Kirkevag, A., Kristjansson, J. E., and Seland, O.: Model intercomparison of indirect aerosol effects, Atmos. Chem. Phys., 6, 3391–3405, 2006, http://www.atmos-chem-phys.net/6/3391/2006/. 14677
Pruppacher, H. R. and Klett, J. D.: Microphysics of Clouds and Precipitation, Kluwer Academic Publishers, 1997. 14687
Roeckner, E., Bäuml, G., Bonaventura, L., Brokopf, R., Esch, M., Giorgetta, M., Hagemann, S., Kirchner, I., Kornblueh, L., Manzini, E., Rhodin, A., Schlese, U., Schulzweida, U., and Tompkins: The atmospheric general circulation modell ECHAM5, Part I: Model description, Tech. Rep. 349, Max-Planck-Institute for Meteorology, Hamburg, Germany, 2003. 14680
Rogers, R. R., Baumgardner, D., Ethier, S. A., Carter, D. A., and Ecklund, W. L.: Comparison of raindrop size distributions measured by radar wind profiler and by airplane, J. Appl. Meteorol., 32, 694–699, 1993. 14685, 14702
Rosenfeld, D., Lahav, R., Khain, A., and Pinsky, M.: The role of sea spray in cleansing air pollution over ocean via cloud processes, Science, 297, 1667–1670, 2002. 14677
Rotstayn, L. D.: A physically based scheme for the treatment of stratiform clouds and precipitation in large-scale models .1. Description and evaluation of the microphysical processes, Q. J. R. Meteorol. Soc., 123, 1227–1282, 1997. 14678
Smolarkiewicz, P. K. and Margolin, L. G.: On forward-in-time differencing for fluids: An Eulerian/semi-Lagrangian nonhydrostatic model for stratified flows, Atmos-Ocean Special, 35, 127–157, 1997. 14679
Smolarkiewicz, P. K. and Margolin, L. G.: MPDATA: A finite-difference solver for geophysical flows, J. Comput. Phys., 140, 459–480, 1998. 14679
Srivastava, R. C.: Parameterization of raindrop size distributions, J. Atmos. Sci., 35, 108–117, 1978. 14683
Stier, P., Feichter, J., Kinne, S., Kloster, S., Vignati, E., Wilson, J., Ganzeveld, L., Tegen, I., Werner, M., Balkanski, Y., Schulz, M., and Boucher, O.: The aerosol-climate model ECHAM5-HAM, Atmos. Chem. Phys., 5, 1125–1156, 2005, http://www.atmos-chem-phys.net/5/1125/2005/. 14680
Storelvmo, T., Kristjansson, J. E., Myhre, G., Johnsrud, M., and Stordal, F.: Combined observational and modeling based study of the aerosol indirect effect, Atmos. Chem. Phys., 6,

3583–3601, 2006, http://www.atmos-chem-phys.net/6/3583/2006/. 14677

Tompkins, A. M.: A prognostic parameterization for the subgrid-scale variability of water vapor and clouds in large-scale models and its use to diagnose cloud cover, J. Atmos. Sci., 59, 1917–1942, 2002. 14680, 14682, 14688

Twomey, S.: Pollution and planetary albedo, Atmos. Environ., 8, 1251–1256, 1974. 14677

Wood, R.: Drizzle in stratiform boundary layer clouds. Part II: Microphysical aspects, J. Atmos. Sci., 62, 3034–3050, 2005. 14677

Xu, K. M., Zhang, M. H., Eitzen, M. A., Ghan, S. J., Klein, S. A., Wu, X. Q., Xie, S. C., Branson, M., Genio, A. D. D., Iacobellis, S. F., Khairoutdinov, M., Lin, W. Y., Lohmann, U., Randall, D. A., Somerville, R. C. J., Sud, Y. C., Walker, G. K., Wolf, A., Yio, J. J., and Zhang, J. H.: Modeling springtime shallow frontal clouds with cloud-resolving and single-column models, J. Geophys. Res.-Atmos., 110, D15S04, 2005. 14680, 14692, 14693

Yanai, M., Esbensen, S., and Chu, J. H.: Determination of bulk properties of tropical cloud clusters from large-scale heat and moisture budgets, J. Atmos. Sci., 30, 611–627, 1973. 14692

Table 1. Mean values of precipitation, cloud cover, LWP, RWP and TWP averaged over the whole simulation period for EPIC from observations (obs) and from simulations with the standard ECHAM5-HAM (std) as well as with ECHAM5-RAIN for different sub-time steps (3,10,30 and 100).

		obs	std	3	10	30	100
precipitation							
cloud base	[$mm\,d^{-1}$]	0.6906	0.3088	0.3064	0.3418	0.3525	0.3566
surface	[$mm\,d^{-1}$]	0.1878	0.1260	0.1146	0.1367	0.1446	0.1459
LWP	[$kg\,m^{-2}$]	–	0.0651	0.0580	0.0497	0.0466	0.0456
RWP	[$kg\,m^{-2}$]	–	0.0000	0.0003	0.0026	0.0040	0.0046
TWP	[$kg\,m^{-2}$]	0.1021	0.0651	0.0583	0.0523	0.0506	0.0502
Cloud cover	[%]	94.0471	72.2656	71.9311	71.4981	71.1928	71.1269

ACPD

7, 14675–14706, 2007

Table 2. Same as Table 2 but for the ARM IOP for different sub-time steps (10, 30, 100 and 300).

		obs	std	10	30	100	300
precipitation surface	[mm d^{-1}]	7.2932	7.5194	7.6481	7.6990	7.7350	7.7460
LWP	[kg m^{-2}]	–	0.1223	0.0687	0.0685	0.0675	0.0675
RWP	[kg m^{-2}]	–	0.0000	0.0176	0.0445	0.0671	0.0750
TWP	[kg m^{-2}]	0.2436	0.1223	0.0863	0.1130	0.1346	0.1425
Cloud cover	[%]	49.5893	75.8476	74.9905	75.3228	75.0800	75.1637

ACPD

7, 14675–14706, 2007

Title Page

Abstract | Introduction

Conclusions | References

Tables | Figures

Back | Close

Full Screen / Esc

Printer-friendly Version

Interactive Discussion

EGU

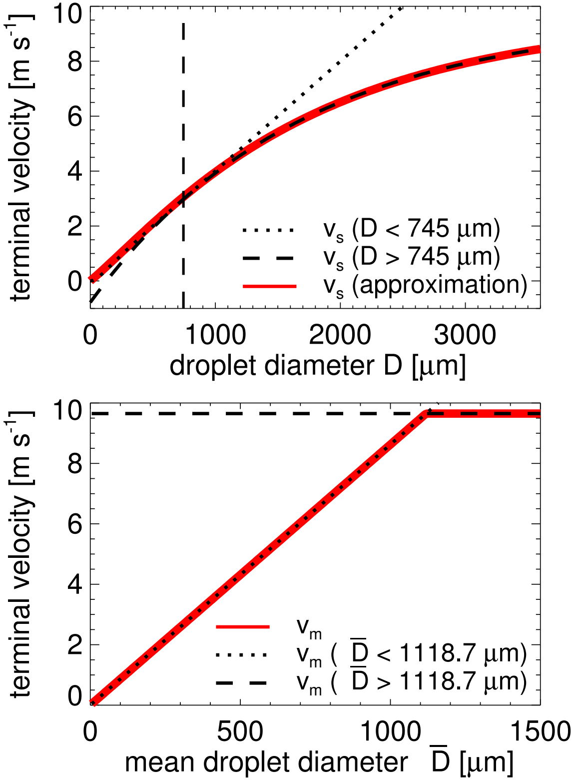

Fig. 1. Terminal velocity: The terminal velocity after Rogers et al. (1993) for small and large drops with the approximation for the whole size range Eq. (11) = red curve (upper panel); the fall velocity for the bulk mass and the bulk number concentration Eq. (12) (lower panel)

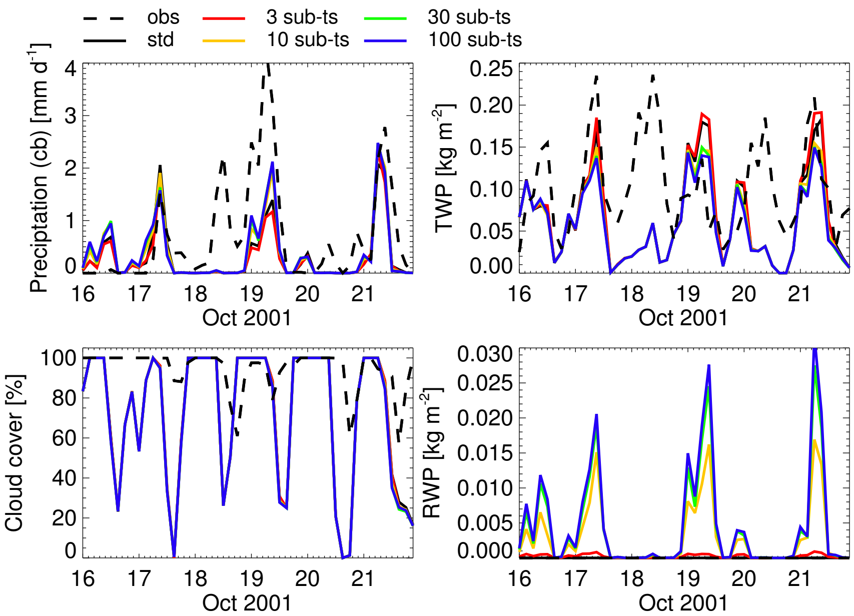

Fig. 2. Precipitation at cloud base (upper left panel), total cloud cover (lower left panel), total liquid water path (upper right panel) and rain water path (lower right panel) from observations during EPIC 2001 (obs) and simulations with ECHAM5-HAM (std) as well as ECHAM5-RAIN for different sub-time steps (3, 10, 30 and 100).

ACPD
7, 14675–14706, 2007

Introduction of prognostic rain in ECHAM5

R. Posselt and U. Lohmann

EGU

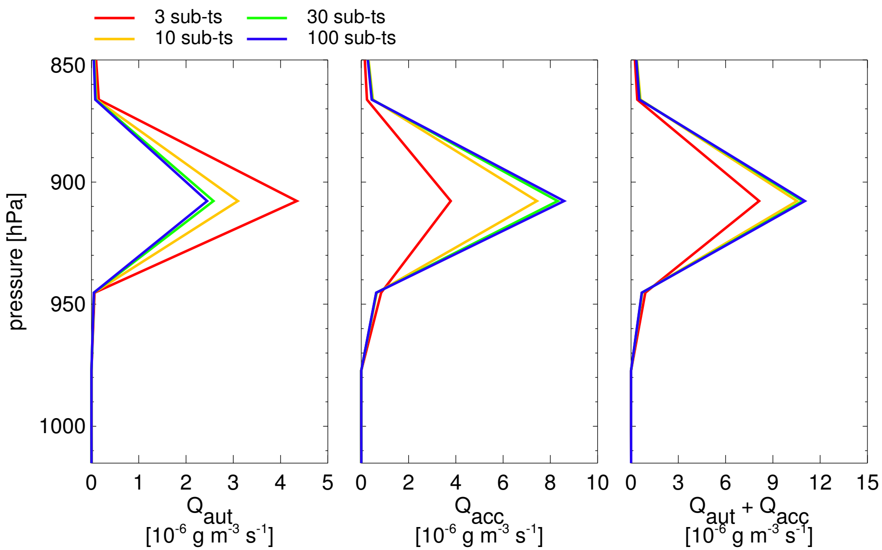

Fig. 3. Vertical profiles of the autoconversion (left panel), accretion (middle panel), and evaporation (right panel) rates from simulations with the ECHAM5-RAIN for different sub-time steps (3, 10, 30 and 100) averaged over the whole EPIC 2001 period.

ACPD

7, 14675–14706, 2007

Introduction of prognostic rain in ECHAM5

R. Posselt and U. Lohmann

EGU

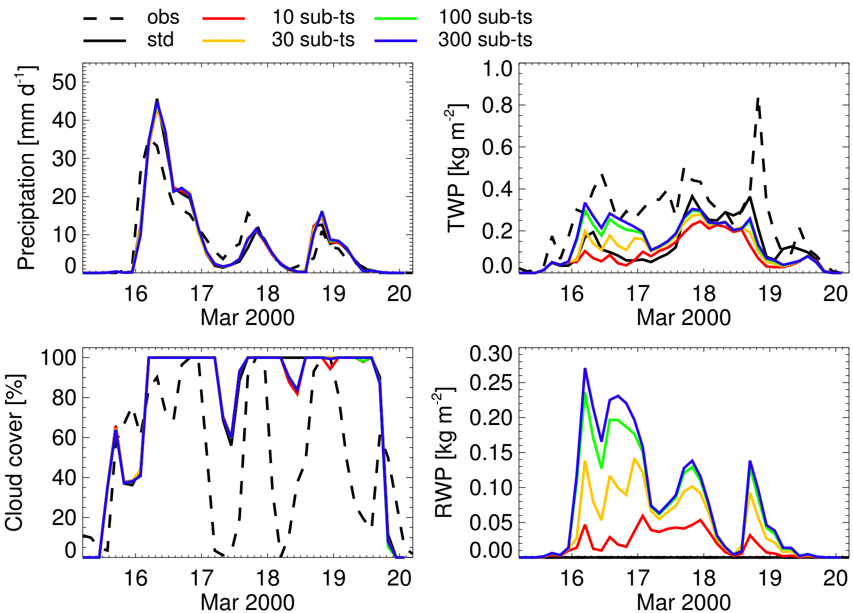

Fig. 4. Precipitation at cloud base (upper left panel), total cloud cover (lower left panel), total liquid water path (upper right panel) and rain water path (lower right panel) from observations during the ARM Cloud IOP (obs) and simulations with ECHAM5-HAM (std) as well as ECHAM5-RAIN for different sub-time steps (10, 30, 100 and 300).

ACPD

7, 14675–14706, 2007

Introduction of prognostic rain in ECHAM5

R. Posselt and U. Lohmann

EGU

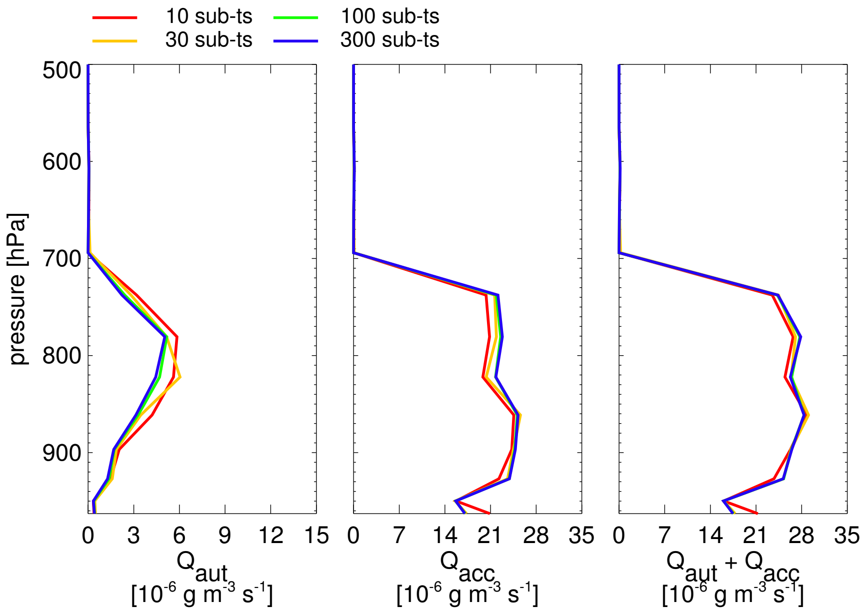

Fig. 5. Vertical profiles of the autoconversion (left panel), accretion (middle panel), and evaporation (right panel) rates from simulations with the ECHAM5-RAIN for different sub-time steps (10, 30, 100 and 300) averaged over the whole ARM IOP period .

ACPD
7, 14675–14706, 2007